Fish and Shellfish Immunology 107 (2020) 95–103

Contents lists available at ScienceDirect

Fish and Shellfish Immunology

journal homepage: www.elsevier.com/locate/fsi

Full length article

Both quiescent and proliferating cells circulate in the blood of the invasive apple snail *Pomacea canaliculata*

Cristian Rodriguez [a,b,c,1], Valeska Simon [d], Paulette Conget [d,**], Israel A. Vega [a,b,c,1,*]

[a] *IHEM, CONICET, Universidad Nacional de Cuyo, Mendoza, Argentina*
[b] *Universidad Nacional de Cuyo, Facultad de Ciencias Médicas, Instituto de Fisiología, Mendoza, Argentina*
[c] *Universidad Nacional de Cuyo, Facultad de Ciencias Exactas y Naturales, Departamento de Biología, Mendoza, Argentina*
[d] *Centro de Medicina Regenerativa, Facultad de Medicina Clínica Alemana Universidad del Desarrollo, 7710162, Santiago, Chile*

ARTICLE INFO

Keywords:
Hematopoiesis
Stem cell
Hemocyte transfer
Cell cycle
Mitochondrial membrane potential
Multixenobiotic resistance system
Angiostrongylus cantonensis
Invasive species

ABSTRACT

Gastropod hematopoiesis occurs at specialized tissues in some species, but the evidence also suggests that hemocyte generation is maybe widespread in the connective tissues or the blood system in others. In Ampullariidae (Caenogastropoda), both the kidney and the lung contain putative hematopoietic cells, which react to immune challenges. In the current study, we wanted to explore if hematopoiesis occurs in the blood of *Pomacea canaliculata*. Thus, we obtained circulating hemocytes from donor animals and tested their ability to proliferate in the blood of conspecific recipients. We tracked cell proliferation by labeling the donors' hemocytes with the fluorescent cell proliferation marker carboxyfluorescein diacetate succinimidyl ester (CFSE). Transferred CFSE-labeled hemocytes survived and proliferated into the recipients' circulation for at least 17 days. We also determined the cell cycle status of circulating hemocytes by using the propidium iodide (PI) and acridine orange (AO) staining methods. Flow cytometry analyses showed that most PI-stained hemocytes were in the G1 phase (~96%), while a lower proportion of cells were through the G2/S-M transition (~4%). When we instead used AO-staining, we further distinguished a subpopulation of cells (~5%) of low size, complexity-granularity, and RNA content. We regarded this subpopulation as quiescent cells. In separate experimental sets, we complemented these findings by assessing in circulating hemocytes two evolutionary conserved features of quiescent, undifferentiated cells. First, we used JC-1 staining to determine the mitochondrial membrane potential (Ψ_m) of circulating hemocytes, which is expected to be low in quiescent cells. Most hemocytes (~87%) showed high aggregation of JC-1, which indicates a high Ψ_m. Besides that, a small hemocyte subpopulation (~11%) showed low aggregation of the dye, thus indicating a low Ψ_m. It is known that the transition from a quiescent to a proliferating state associates with an increase of the Ψ_m. The specificity of these changes was here controlled by membrane depolarization with the Ψ_m disruptor CCCP. Second, we stained hemocytes with Hoechst33342 dye to determine the efflux activity of ABC transporters, which participate in the multixenobiotic resistance system characteristic of undifferentiated cells. Most hemocytes (>99%) showed a low dye-efflux activity, but a small proportion of cells (0.06–0.12%) showed a high dye-efflux activity, which was significantly inhibited by 100 and 500 μM verapamil, and thus is indicative of an undifferentiated subpopulation of circulating hemocytes. Taken together, our results suggest that, among circulating hemocytes, there are cells with the ability to proliferate or to stay in a quiescent state and behave as progenitor cells later, either in the circulation or the hematopoietic tissues/organs.

1. Introduction

Pomacea canaliculata is a caenogastropod that has acquired international notoriety because of its invasiveness [1,2] and its role as an intermediate host for *Angiostrongylus cantonensis*, the nematode that causes eosinophilic meningitis, a rarely fatal but frequently disabling

* Corresponding author. Laboratorio de Fisiología (IHEM-CONICET). Casilla de Correo 33. 5500. Mendoza, Argentina.
** Corresponding author. Centro de Medicina Regenerativa, Facultad de Medicina Clínica Alemana Universidad del Desarrollo. Santiago, Chile.
E-mail addresses: pconget@udd.cl (P. Conget), ivega@mendoza-conicet.gob.ar, iavega.conicet@gmail.com (I.A. Vega).
[1] These authors contributed equally to this work.

https://doi.org/10.1016/j.fsi.2020.09.026
Received 16 June 2020; Received in revised form 13 September 2020; Accepted 17 September 2020
Available online 20 September 2020

zoonotic disease [3–5]. Because of this association, the cellular components of the internal defense system of *P. canaliculata*, i.e., the hemocytes, have become the focus of attention over the past few years [6–13].

P. canaliculata hemocytes may circulate freely in the blood but some become resident or 'fixed' in tissues, such as in the renal islets [10,12] or the gill epithelium [13]. Adult, previously undisturbed individuals of this species show a circulating hemocyte concentration of ~3×10^6 cells/mL [11,14]. This concentration is supposed to be a basal estimation that may fluctuate as a consequence of cell death, cell generation, and cell migration to and from the hemocyte reservoirs in the kidney islets or in hemocyte nodules that form in the lung and other tissues after immune challenges [10,12]. Three hemocyte 'types' with different circulating concentrations are found in the basal condition (hyalinocytes, 63.0 ± 3.8%; granulocytes, 8.9 ± 2.6%; agranulocytes, 28.1 ± 1.6%). They have been morphologically and functionally characterized by Ref. [10]: hyalinocytes seem mainly involved in phagocytosis of intruders, while granulocytes may exocytose their granules which would contain lytic substances, as shown by Ref. [15] in another gastropod species. A kind of "compound exocytosis" (sensu [16]) may also occur in *P. canaliculata* granulocytes [10]. Agranulocytes, in turn, are cells with a scarce cytoplasm, small mitochondria, and that are practically devoid of cytoplasmic granules [10]. Some agranulocytes are supposed to be "blast-like" cells [7], which may account for hematopoietic events in the blood, as observed in other gastropods [17]. Hematopoiesis should occur continuously to replace senescent and/or dead hemocytes, the generation rate of these cells should fluctuate more than most others, particularly in response to immune challenges [18].

An all-encompassing, comparative view of hematopoiesis in the widely diverse class Gastropoda is still wanting. Indeed, studies have been restricted to seven families of Heterobranchia (namely, Bradybaenidae, Bulinidae, Lymnaeidae, Physidae, Planorbidae, Philomycidae and Strophocheilidae) and a single family of Caenogastropoda (Ampullariidae, to which *P. canaliculata* belongs to). Therefore, our comparative knowledge of gastropod hematopoiesis should be considered as quite fragmentary. With this limitation in mind, we will only state that there are gastropod species in which hematopoiesis occurs localized in specialized tissues/organs [19–25] or widespread in the connective tissue or even in the entire blood system in others [20,24,26–28]. Indeed, *P. canaliculata* could be included among the species in which localized hematopoiesis occurs, because both basal and stimulated hemocyte proliferation was quantified in renal hemocyte islets after an immune challenge [12].

However, in the current study, we wanted to explore the possibility of hemocyte generation in the circulating blood of *P. canaliculata*. We first transferred to *P. canaliculata* individuals hemocytes obtained from conspecific donors and that were labeled with carboxyfluorescein diacetate succinimidyl ester (CFSE), and we later checked these hemocytes for survival and proliferation in the circulation [29]. In separate experimental sets, we complemented this by assessing stem cell-like features [30] in the circulating hemocytes of *P. canaliculata*. We searched for circulating hemocyte populations showing differences in: (1) the nucleic acid contents, estimated by employing the flow cytometry propidium iodide (PI) method [31], refined by the use of the metachromatic fluorochrome acridine orange (AO), which allowed the simultaneous analysis of DNA and RNA contents [32] and the distinction of hemocytes in different stages of the cell cycle, (2) the aggregation of the fluorescent probe 5,5′,6,6′-tetrachloro-1,1′,3,3′-tetraethylbenzimidazolylcarbocyanine iodide (JC-1), which allowed us to estimate the mitochondrial membrane potential (Ψ_m) [33,34] that is expected to be low in quiescent cells [35], and (3) the ability to extrude the fluorochrome Hoechst33342 (H33342) as indicative of the expression of ABC transporters' genes, which is a feature of undifferentiated cells [36–38].

2. Materials and methods

2.1. Animals and culturing conditions

Adult *P. canaliculata* snails (11–14 g) were obtained from our Rosedal strain, the origin and culture conditions of which have been reported previously (e.g., Ref. [10,12]). Briefly, the animals were kept in aquaria under controlled temperature (24–26 °C) and photoperiod (14:10 light/dark cycle) and fed ad libitum with a diet composed of fresh lettuce, carp food pellets (Peishe Car Shulet, Argentina), powdered *P. canaliculata*'s eggs (as a protein and calcium supplement), and toilet paper (Higienol®, Argentina).

2.2. Blood collection

The shell of each snail was cleaned and dried with tissue paper to avoid contamination of the blood samples. Unless repeated blood collections from the same snail were needed (see Section 2.4.3), a small opening was made near the shell umbilicum, and the pericardium was opened to expose the heart ventricle, from which 0.5–1 mL of blood was collected using a plastic syringe moistened with an antiaggregant buffered saline solution (*Pc*ABS: 43 mM NaCl, 1.8 mM KCl, 30 mM EDTA, 10 mM HEPES; pH = 7.6) designed to match the osmolality and pH of *P. canaliculata*'s plasma [10].

2.3. Total hemocyte count and cell viability

After each blood withdrawal, both total hemocyte count and viability were recorded. The total hemocyte count was determined by flow cytometry following the procedure described by Ref. [39]. Briefly, blood samples diluted with phosphate-buffered saline (~140 mOsm; hereafter referred to as PBS) containing 1×10^5 beads (6.0 μm in diameter; Count Bright Beads, Invitrogen) were analyzed in either a CyAn ADP (Dako–Carpinteria, California–USA) or a FACS Aria II (Becton–Dickinson, San José, California–USA) flow cytometer. A dot plot of forward light scatter (FSC) *vs* side light scatter (SSC), indicating differences in cell size and internal complexity, was used to frame two regions: (R1) hemocytes gate and (R2) beads gate (Fig. 1A–B). The absolute number of hemocytes per mL of blood was calculated as: (number of events in R1/number of events in R2) × (1×10^5 [total beads in tube; from manufacturer] × 10 [inverse of the sample dilution]).

Hemocyte viability was assessed by flow cytometry, using the propidium iodide (PI) exclusion method [40]. Briefly, 5 μL of 1 mg/mL PI (Molecular Probes, Invitrogen) was added to live cell suspensions immediately before flow cytometry analysis. Excitation was made with an argon ion laser at 488 nm and signals of size (FS), internal complexity (SS), and PI fluorescence (FL3) were captured. Twenty thousand events per sample were recorded. Dot plots of FL3 *vs* SS were used to record cell viability. The viability of hemocytes obtained from the heart was ~99% (Fig. 1C–D).

Flow cytometry analysis of circulating hemocytes obtained from adult animals. **(A)** Representative sample of control circulating hemocytes (R1) showing their variation in size (FS) and complexity-granularity (SS); 6 μm-beads (R2) were used to quantify the hemocyte number. **(B)** Dot plots of FS *vs* Pulse Width were used to select single hemocytes, discarding doublets or triplets from further analysis. **(C)** Dot plot showing the frame used to distinguish the non-viable (PI^+) from the viable cells. **(D)** Histogram of PI intensity of the same hemocyte sample shown in panel C.

2.4. Conspecific transfer of CFSE-labeled hemocytes

We showed the self-renewal ability *in vivo* of the circulating hemocytes by the transfer of hemocytes fluorescently labeled with CFSE [29], which has been used to track *in vivo* proliferating cells in mice. As CFSE divides equally between daughter cells, successive rounds of cell

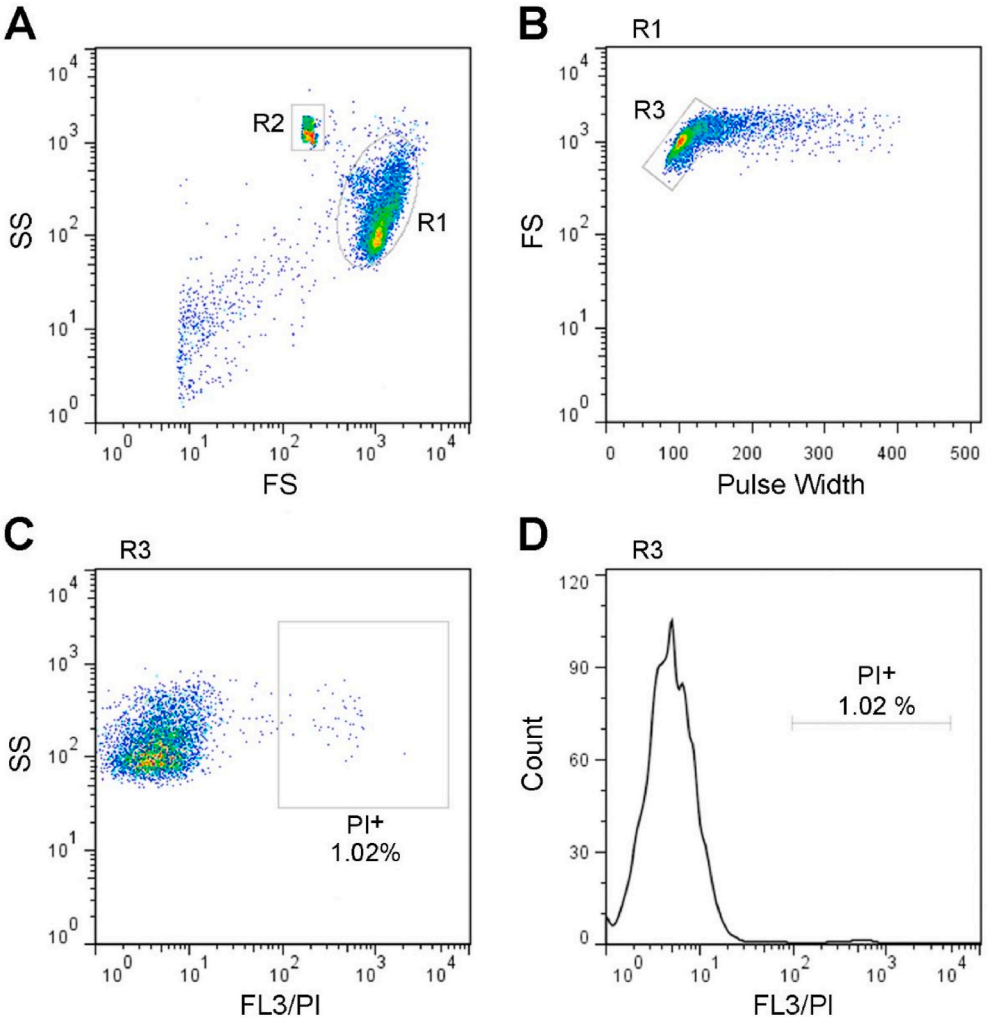

Fig. 1. Total hemocyte count and cell viability.

division can be determined by flow cytometry [41].

2.4.1. In vitro CFSE labeling of hemocytes

Blood samples were centrifuged (700×*g*) at 4 °C for 10 min, and the hemocyte pellet was suspended in *Pc*ABS. Hemocytes were pooled and incubated with 1 μmol/L CFDA-SE (Cell Trace™ CFSE Cell Proliferation Kit, Invitrogen) in *Pc*ABS at room temperature for 10 min to yield CFSE by intracellular esterase activity. Then, samples were analyzed in a FACSAria III flow cytometer (Becton–Dickinson Bioscience, California, USA) to confirm CFSE labeling and adjust the CFSE fluorescence parameter. The hemocyte population was gated to exclude cell debris and cell doublets, and dot plots of SS *vs* FL1 (CFSE) were used to identify CFSE-labeled cells (i.e., $CFSE^+$ cells; Suppl. Fig. S1). The maximum CFSE fluorescence was set to 10^5 arbitrary units.

As DMSO is frequently used as an inhibitor for cell division in mice models (e.g., Ref. [42]), we additionally incubated hemocytes with 1 μmol/L CFDA-SE and 10% DMSO (CFSE/DMSO-labeled hemocytes). Cell labeling was stopped by diluting samples with 2 mL of *Pc*ABS, containing 10% cell-free blood plasma, at 4 °C for 5 min.

2.4.2. Conspecific transfer of CFSE-labeled hemocytes

CFSE labeled-cell samples were centrifuged (700×*g*) for 5 min at 4 °C, and the cells were suspended in *Pc*BS. Finally, an inoculum of 200 μL of *Pc*BS containing 1.5×10^6 CFSE- or CFSE/DMSO-labeled hemocytes was injected into the foot of recipient snails (N = 3). Three additional snails were injected with the same number of unlabeled hemocytes as a control for autofluorescence.

Suppl. Fig. S1. Hemocytes gate selection and CFSE fluorescence adjustment after *in vitro* labeling.

Flow cytometry analysis of CFSE-labeled hemocytes obtained from donor animals. **(A)** Representative sample of circulating hemocytes showing their variation in size (FSC) and internal complexity (SSC). **(B)** Dot plot of FS *vs* Pulse Width were used to select single hemocytes. **(C)** Dot plot of CFSE-labeled hemocytes. **(D)** Histogram of $CFSE^+$ cells from panel C, adjusted to 10^5 (arbitrary units).

2.4.3. Repeated blood sampling

Repeated blood withdrawals were performed at 3, 6, 9, and 17 days after the transfer of CFSE-labeled hemocytes by gently pushing the operculum to induce exsanguination through the "blood pore" [7,43,44]; prior to blood withdrawals, the animal shells were cleaned as described in Section 2.2. Blood samples thus obtained were filtered through a cell-strainer (35 μm, Falcon, Becton Dickinson), collected on Petri dishes, and immediately diluted with 1 mL of *Pc*ABS to prevent hemocyte adhesion/aggregation. All blood samples were analyzed by flow cytometry.

2.4.4. Flow cytometry analysis of circulating hemocytes in recipient animals

As different hemocyte types circulate in the blood [10] and they may show different labeling or division kinetics, we did not attempt to distinguish individual peaks of CFSE intensity (as it is customary for analyzing CFSE data). Instead, we classified the hemocytes as $CFSE^+$ or

$CFSE^-$, and recorded the proportion of $CFSE^+$ cells (see Refs. [45,46]), along the different sampling times (3, 6, 9, and 17 days post-injection) in the CFSE, CFSE/DMSO, and control (autofluorescence) groups (Suppl. Fig. S2).

Suppl. Fig. S2. Flow cytometry analysis of recipients' hemocytes after the conspecific transfer of CFSE-labeled cells. Dot plots showing the frames used to classify $CFSE^-$ and $CFSE^+$ cells in the CFSE, CFSE/DMSO, and control (autofluorescence) groups.

2.5. Cell cycle of circulating hemocytes

To determine the cell cycle of circulating hemocytes, we used the propidium iodide (PI) flow cytometric assay, which has been widely used in different experimental models [31,40]. By using this method, it was possible to identify circulating hemocytes in the different phases of the cell cycle (G1, S, and G2–M). A complementary approach based on the simultaneous analysis of DNA and RNA contents by using the metachromatic fluorochrome acridine orange (AO), which was useful to further distinguish G1 from G1q (quiescent) cells [32].

2.5.1. Identification of cell cycle phases by PI-staining

Blood samples were centrifuged (700×*g*) for 10 min at 4 °C, and the hemocytes thus obtained were fixed with ice-cold 70% ethanol for 20 min. Then, ~5×10^5 fixed cells were suspended and stained with 50 μg/mL PI in a 0.1% sodium citrate solution containing 200 μg/mL ribonuclease A, for 30 min at room temperature. Samples were analyzed by flow cytometry, and dot plots of either size (FS) or internal complexity (SS) *vs* PI fluorescence (FL3) were used to identify the different phases of the cell cycle (G1, G1q, and S/G2–M). Additionally, the DNA content was quantified (median fluorescence intensity, MFI) and compared between the phases G1 and S/G2–M ($P \leq 0.05$, Mann–Whitney *U*-test). Data were given as mean ± SEM for each group (N = 4).

2.5.2. Identification of quiescent, non-cycling cells by AO-staining

Hemocytes were further classified based on the differential staining of DNA and RNA with AO, following the procedure by Ref. [32]. For this purpose, 2×10^5 live cells were incubated in 200 μL of an acidic saline solution (150 mM NaCl, 60 mM HCl, 0.1% Triton X-100; pH = 1.2) for 15 s and in saline citrate–phosphate buffer (37 mM citric acid, 126 mM NaH2PO4, 1 mM EDTA, 150 mM NaCl; pH = 6) containing 0.6 μg/mL AO for 4 min. All steps were performed at 4 °C to prevent DNA denaturation and hemocyte aggregation.

DNA–AO and RNA–AO complexes were detected by flow cytometry. Dot plots of DNA (green fluorescence, FL1) *vs* RNA (red fluorescence, FL3) were used to identify quiescent, non-cycling G1q cells, while distinguishing them from those entering the cell cycle, as described by Ref. [32]. Small cells (FS^{low}) with low RNA content (RNA^{low}) were regarded as G1q cells. Also, because it was assumed that an increase in both DNA and RNA contents parallels the progression through the cell cycle [32], large (FS^{high}) hemocytes with high RNA content (RNA^{high}) were regarded as active-cycling cells. Additionally, the RNA content was quantified (arbitrary fluorescence units) and compared between quiescent and active-cycling cells ($P \leq 0.05$, Mann–Whitney *U*-test). Data were given as mean ± SEM (N = 3 per group). Statistical analysis was performed with GraphPad Prism v.5.00 (GraphPad Software, San Diego, California, USA).

2.6. Assessment of mitochondrial membrane potential (Ψ_m)

This was made by using 5,5′,6,6′-tetrachloro-1,1′,3,3′-tetraethylbenzimidazolylcarbocyanine iodide (JC-1) fluorescent cation staining (MitoProbe™ JC-1 Assay Kit for Flow Cytometry; M34152) [33,34]. As JC-1 monomers accumulate in the mitochondrial matrix and aggregate as a consequence of high Ψ_m, their emission spectrum changes from green to red [33,47]. The polymer/monomer ratio is thus an accurate measure of Ψ_m [48], which also takes into consideration both mitochondrial mass and cell size [49]. The specificity of this change is controlled by the exposure of cells to the Ψ_m-disruptor carbonyl cyanide-3-chlorophenylhydrazone (CCCP).

For this purpose, 2×10^5 live cells were incubated in PBS containing 2 μM JC-1 for 120 min. Control cells were incubated with 2 μM JC-1 and 50 μM CCCP to depolarize mitochondria. Dot plots of green (FL1) *vs* red (FL2) fluorescence were used to identify live cells with either a low or high Ψ_m. Then, the red/green ratio was quantified (arbitrary fluorescence units) and compared between the two subpopulations ($P \leq 0.05$, Mann–Whitney *U*-test). Data were given as mean ± SEM (N = 4).

2.7. Assessment of H33342-efflux activity

The efflux of DNA-binding Hoechst dyes associates with the expression of ABC transporters and multidrug resistance (MDR) efflux pumps [50,51]. There has been shown that a variety of stem cells express ABC transporters and MDR efflux pumps, which are interpreted as parts of a cellular multixenobiotic resistance (MXR) defense system [51–53]. To assess the ABC transporters' activity of presumptive adult stem cells, we measured the ability of circulating hemocytes to exclude H33342 dye.

For this purpose, 5×10^5 live cells were incubated in *Pc*ABS containing 5 μg/mL of H33342 and maintained for 90 min at 37 °C; samples were gently agitated every 10 min (N = 3). Under these conditions, a dye balance was reached between the extracellular and intracellular media. Additional *P. canaliculata* individuals were exposed to different concentrations of the ABC-transporter inhibitor verapamil (50, 100, and 500 μM; N = 3). Hemocytes were then washed, centrifuged, suspended in the culture medium, and analyzed by flow cytometry to identify those cells able to exclude the dye.

Cells with a high efflux pump activity ($H33342^{low}$) were identified at the bottom left corner of the dot plots of blue (FL1) *vs* violet (FL3) fluorescence according to the dual parameter method by Ref. [52] and were recorded and compared between groups. The percent inhibition of ABC transporters by verapamil was also recorded in hemocytes with high efflux pump activity ($H33342^{high}$). Ninety-nine % confidence intervals were used to assess the significance of differences between groups.

3. Results

3.1. Conspecific transfer of CFSE-labeled hemocytes

CFSE-labeled hemocytes from donor snails were found in blood of all the conspecific recipients and they could be followed by repeated exsanguinations (Suppl. Fig. S2). In the CFSE group, the proportion of $CFSE^+$ cells followed a decreasing trend (Fig. 2A), and the median rate of loss of CFSE-labeled hemocytes during the first six days post-injection was faster than at later time points (0.006%/day *vs* 0.0006%/day). In turn, the proportion of CFSE-labeled cells in the CFSE/DMSO-group did not change in two of the studied animals, but it dropped to zero at the ninth day post-injection in the other studied animal (Fig. 2B).

CFSE histograms were used to track the CFSE profiles in both the CFSE and CFSE/DMSO groups (Fig. 2C–D). At least two peaks of fluorescence intensity were found in the CFSE group, during the observation period, concomitantly with the decrease in cell frequency of the peak of maximum fluorescence intensity (Fig. 2D), and this is indicative of transferred cells' division in the circulation of recipient snails. Also, the occurrence of some peaks of lower fluorescence intensities (e.g., 10^4) indicated that an average $CFSE^+$ cell underwent more than three division cycles. In the CFSE/DMSO group, no lower fluorescence intensity peaks were found, and the peak of maximum intensity did not decrease in height. A time-dependent decrease in the fluorescence intensity of CFSE was seen in the two groups (Fig. 2C–D, dashed lines).

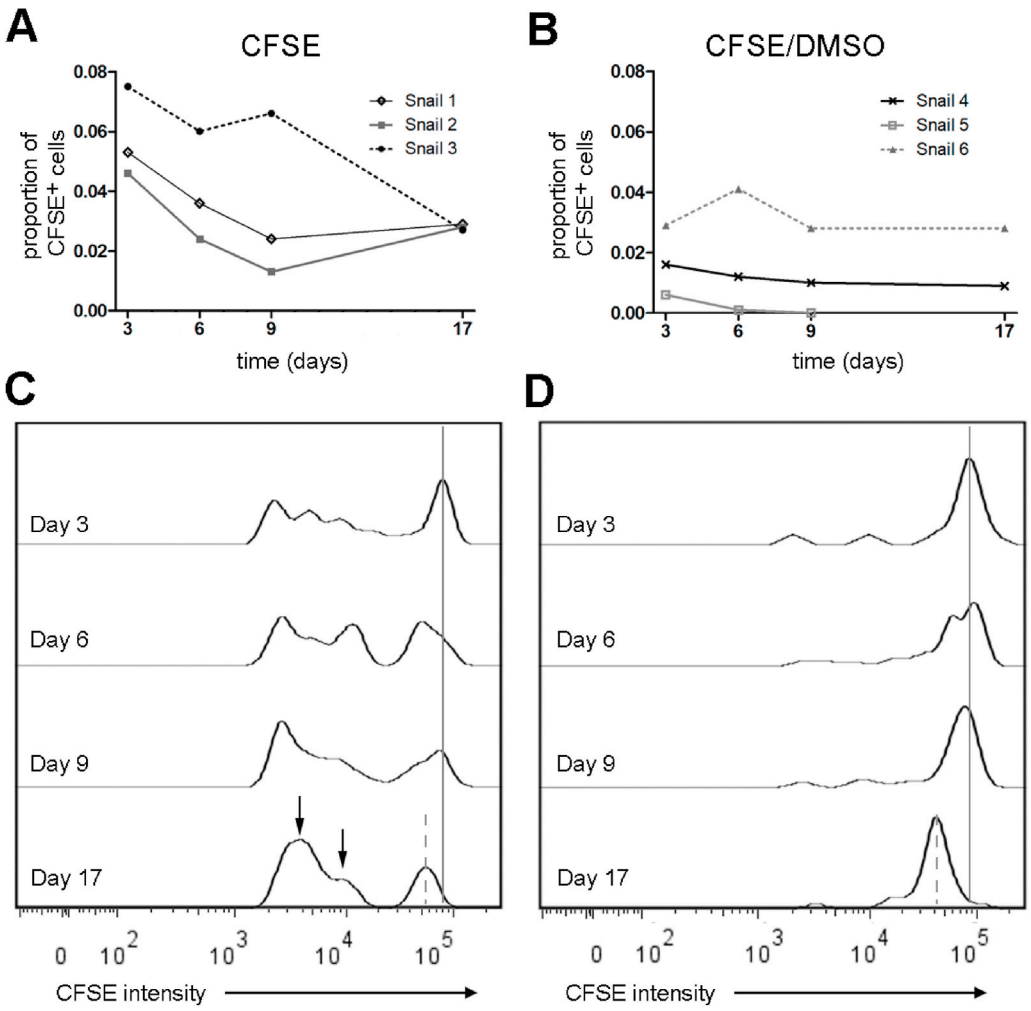

Fig. 2. Transfer of conspecific CFSE-labeled hemocytes. (A) Proportion of $CFSE^+$ cells through time in the CFSE group. **(B)** Proportion of $CFSE^+$ cells through time in the CFSE/DMSO group. **(C)** Histogram of $CFSE^+$ cells showing temporal changes in blood of a representative recipient snail. Arrows indicate distinct fluorescence peaks on day 17 after transfer. **(D)** Histogram of $CFSE^+$ cells showing temporal changes after repeated exsanguinations of a representative recipient snail in the CFSE/DMSO group. No distinct fluorescence peaks are found. The solid line indicates the peak of maximum CFSE fluorescence intensity ($\sim 10^5$), and the dashed lines indicate the time-dependent fluorescence decay in the two groups (CFSE and CFSE/DMSO).

3.2. Cell cycle of circulating hemocytes

The PI-staining method showed that most circulating hemocytes (96 ± 2%) were in the G1 phase, whereas a lower percentage of cells was found in phases S/G2-M (4 ± 2%; Fig. 3A). Also, the two subpopulations differed significantly in their DNA contents (Fig. 3B).

The AO-staining method showed three circulating hemocyte subpopulations, which differed according to their nucleic acids contents (Fig. 4A): two low RNA content cell subpopulations (G1 and G1q cells), which differed in size, and a third subpopulation with high DNA and RNA contents (S/G2–M cells). Small cells with low RNA content were interpreted as quiescent, non-cycling cells, and they represented 5.0 ± 0.9% of the circulating hemocytes, while cycling S/G2-M cells comprised 7 ± 3% of the hemocyte population. G1q cells had an average

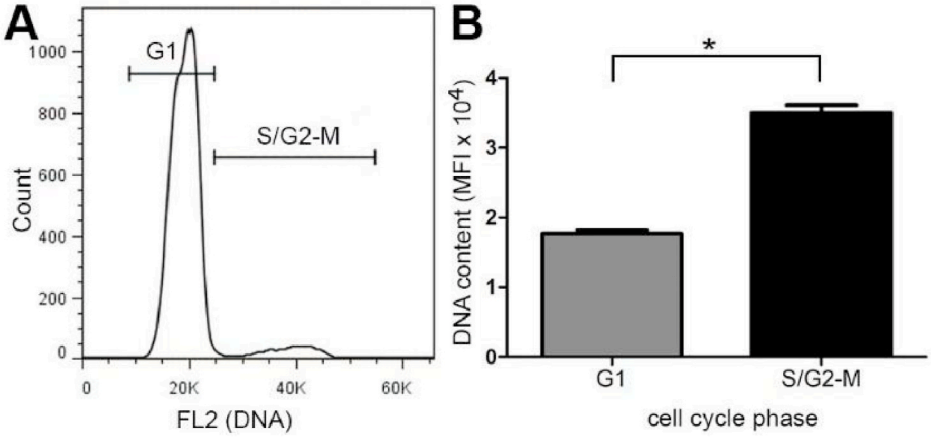

Fig. 3. Cell cycle in circulating hemocytes (PI-staining). (A) Representative histogram of DNA fluorescence showing the marks used to distinguish G1 from S/G2-M hemocytes. **(B)** Relative comparison of DNA content (arbitrary units) between hemocytes in the G1 and S/G2-M phases. MFI, median fluorescence intensity. Data are shown as mean ± SEM. *$P < 0.05$ (Mann–Whitney U-test; N = 4).

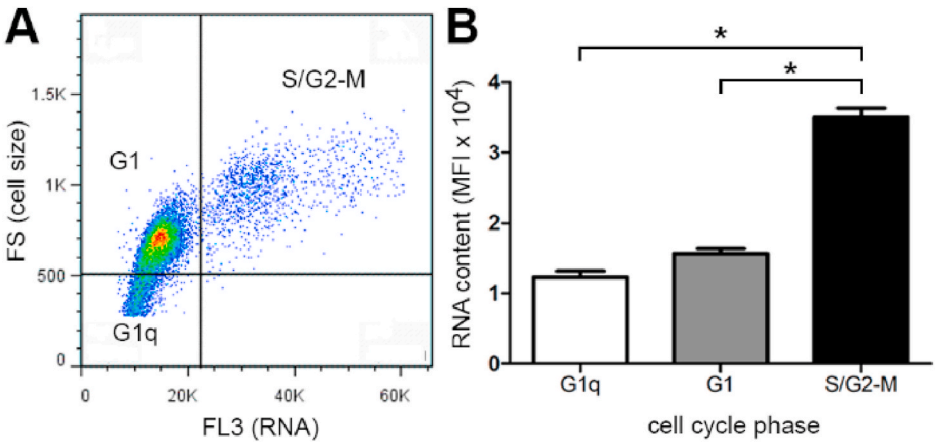

Fig. 4. Circulating hemocyte subpopulations: non-cycling cells (G1 and G1q) are distinguished from the active-cycling (S/G2–M) cells by AO-staining. (A) Dot plot of FS (cell size) *vs* FL3 (RNA fluorescence) showing the three subpopulations. **(B)** Relative RNA contents (median fluorescence intensity in arbitrary units) of G1, G1q and S/G2-M cells. Data are shown as mean ± SEM. *$P < 0.05$ (Mann–Whitney *U*-test, N = 3).

~4 times less RNA content than cycling S/G2-M cells, although showed no difference with G1 cells (Fig. 4B).

3.3. Mitochondrial membrane potential of circulating hemocytes

Most hemocytes (~87%) showed high JC-1 dye accumulation (high green fluorescence) and aggregation (high red fluorescence) (Fig. 5A; upper right quadrant). Besides, a small proportion of hemocytes (~11%) showed high accumulation (high green fluorescence), but low aggregation (low red fluorescence), thus indicating a low mitochondrial membrane potential (Ψ_m^{low}) (Fig. 5A; lower right quadrant). Hemocytes did not neither accumulate (low green fluorescence) nor aggregate (low red fluorescence) JC-1 stain when they were exposed to the mitochondrial membrane potential disruptor, CCCP (Fig. 5B; lower left quadrant). The changes found in the two hemocyte populations (Ψ_m^{high} and Ψ_m^{low}) were those only associated with the formation of JC-1 aggregates (Fig. 5C), because there was no statistically significant difference in the accumulation of JC-1 monomers ($P > 0.05$, Mann–Whitney *U*-test).

3.4. H33342 efflux activity of circulating hemocytes

Most of the circulating hemocytes (>99%) had low or null H33342 dye-efflux ability. However, a very-small cell population (0.06–0.12%) showed a high dye-efflux pump activity (P4 region, Fig. 6A and B). Verapamil caused a significant inhibitory effect on total H33342-efflux activity in P4 cells exposed to 100 and 500 μM verapamil (99% confidence intervals, Fig. 6C).

4. Discussion

Our knowledge about gastropod hematopoiesis may be biased because current evidence comes almost exclusively from seven families of the clade Heterobranchia. There are few studies on other clades, even the Caenogastropoda, which encompass 60% of the extant gastropod species. Among the latter, only two species of Ampullariidae, namely *Marisa cornuarietis* and *Pomacea canaliculata*, have been studied in this regard [8,12,54]. In both species, the available data suggest that hemocyte production seems localized at defined tissues. In *M. cornuarietis*, it has been reported in the lung roof and the connective tissue [54]. In *P. canaliculata* hematopoiesis was localized in the kidney islets [12]. However, as observations in *M. cornuarietis* and other gastropods suggest, hematopoiesis may also occur widespread in the blood [17].

In this work, we tested the hypothesis of a circulating hemocyte population able to divide in the blood. The transfer of CFSE-labeled hemocytes allowed us to detect proliferating hemocytes in the blood of recipient *P. canaliculata* individuals (Fig. 2), indicating the presence of proliferative hematopoietic cells in the donors' circulation. The different peaks of decreasing fluorescence intensities, found in CFSE-labeled cells from the control group (Fig. 2), corresponded to successive cell divisions in the recipients' circulation. The absence of different fluorescence

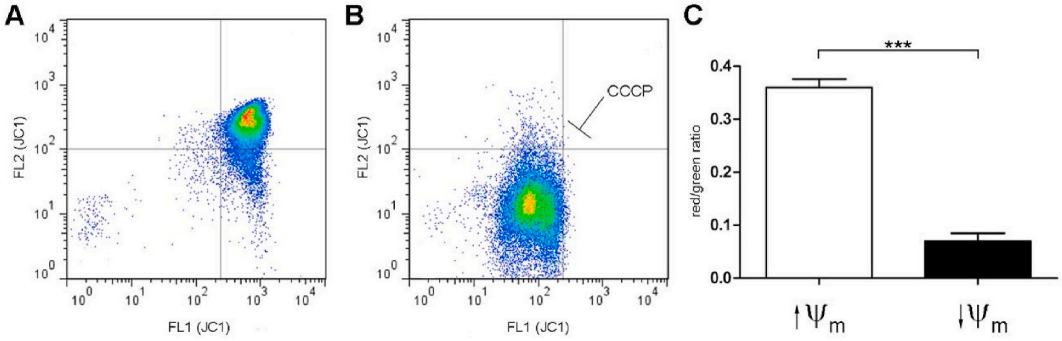

Fig. 5. Mitochondrial membrane potential of circulating hemocytes. (A) The dot plot shows most hemocytes (87%; upper right quadrant) exhibiting high accumulation (green fluorescence, FL1) and aggregation (red fluorescence, FL2) of the dye JC-1; only a smaller subpopulation (11%; lower right quadrant) shows low red fluorescence, indicative of low mitochondrial membrane potential. **(B)** The membrane potential disruptor CCCP depresses both green and red fluorescence, and the difference between both subpopulations disappeared. **(C)** The red/green fluorescence ratio (aggregation/accumulation) shows a significant difference between the two subpopulations evidenced on panel A. Data are shown as mean ± SEM. *$P < 0.05$ (Mann–Whitney *U*-test, N = 4). (For interpretation of the references to colour in this figure legend, the reader is referred to the Web version of this article.)

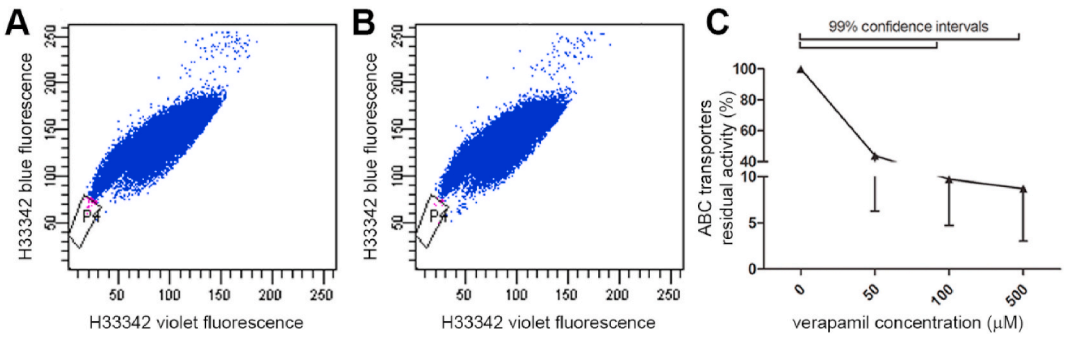

Fig. 6. Hoechst33342 (H33342) dye-efflux activity of circulating hemocytes. (A) Control hemocyte sample showing a subpopulation (P4) with low dye fluorescence, indicating a high dye-efflux activity. **(B)** Hemocytes exposed to verapamil (500 μM), an inhibitor of ABC transporters. **(C)** Percent inhibition (mean ± SEM) of H33342-efflux activity at the different verapamil concentrations tested (0, 50, 100, and 500 μM) in P4 cells. Differences between groups were assessed using 99% confidence intervals (N = 3 per group).

peaks in the CFSE/DMSO group could be indicating inhibition of cell proliferation by DMSO, as was reported for mice leukocytes [42].

The proportion of CFSE-labeled cells dropped fast during the first 6 days after transfer and then decreased 10-fold in the following days (Fig. 2A and B). The rapid loss of cells in the first 6 days may be due to (1) a high death rate of CFSE-labeled hemocytes in the recipient's circulation; (2) a high cell division rate; (3) dilution of CFSE-labeled cells in the circulation because of the migration of native (i.e., unlabeled) cells from hemocyte reservoirs, such as the hemocyte renal islets; or (4) the migration or aggregation of CFSE-labeled cells into organs/tissues. Some of these non-mutually exclusive possibilities have been the subject of mathematical modeling in other experimental animals to estimate proliferation and death rates (e.g., Ref. [45]; for sheep lymphocytes). The third and fourth possibilities refer to the to and fro hemocyte migration between different compartments (e.g., between blood and tissue reservoirs) that would happen in response to different factors such as antigen administration [14] or environmental changes, as shown in the ampullariid *Pila globosa* [55].

We also performed a flow cytometry assessment of the cell cycle of circulating hemocytes, by using both PI- and AO-staining methods, as a more direct approach to explore whether both quiescent and proliferative cells occurred in the circulation. PI-staining showed that most circulating hemocytes were found in G1 phase (~96%), while a lower proportion of cells were between S and G_2–M phases (Fig. 3). In turn, when using AO-staining (Fig. 4), we distinguished different hemocyte subpopulations in the circulation, based on cell size, complexity–granularity, and RNA content. Among these subpopulations, this procedure allowed us to further distinguish a 5%-subpopulation of quiescent hemocytes (G1q) from two others subpopulation of non-quiescent cells (G1 and S/G2-M, 87% and 7%, respectively).

Together, the CFSE-labeling and cell cycle data support the occurrence of both quiescent and proliferating cells in the circulating blood of *P. canaliculata*. Some of the quiescent hemocytes may move towards differentiation, while a small part may remain in the quiescent state and behave as progenitor cells later, either in the circulation or the hematopoietic tissues/organs.

Furthermore, we wanted to explore whether two conserved stem cell-like features [30] could be detected in circulating hemocyte subpopulations of *P. canaliculata*, namely a low mitochondrial membrane potential and a high ABC transporter dye-efflux capacity, as evidenced by the JC-1 and Hoechst33342 staining methods, respectively.

The pluripotency of stem cells seems strongly associated with a low mitochondrial metabolism [56–60], while the activation of mitochondrial metabolism precedes proliferation and differentiation [49,61]. [49] have taken advantage of this property to purify adult stem cells in mice, using JC-1 as an accurate Ψ_m marker, which normalize data according to mitochondrial mass and cell size.

Our current flow cytometry analysis of circulating hemocytes with JC-1 showed the occurrence of a small population with low Ψ_m (Fig. 5) that may be similar to the "very-small embryonic-like stem cells" of [62]; found in humans, mice and chickens, which show sparse, globular mitochondria, with poorly developed cristae and placed around the nucleus, which has also been reported in other mammalian embryonic stem cells [63–66]. Perinuclear small, round mitochondria with poorly developed cristae, were also observed in *P. canaliculata* [10], but the significance of this cytoplasmic localization is yet uncertain [64]. Notwithstanding, most circulating hemocytes in the current study showed a high, homogenous mitochondrial activity (Ψ_m^{high} = 87%), which is consistent with the occurrence of elongated mitochondria, with well-developed cristae and a dense matrix, frequently observed in circulating hemocytes [10].

Multixenobiotic resistance (MXR) is an important defense system, as it shows a high capacity of efflux for a wide range of environmental pollutants [37]. For instance, in mice, MDR1 has been shown to be an important cause of multidrug resistance in both stem and cancer cells [36]. In the aquatic invertebrates studied in this respect, the role of MXR is acquired from P-glycoprotein (P-gp), Mrp1, and Bcrp, which are members of the ABC transporters superfamily [67,68]. Activity of these ABC proteins can be quantified by the accumulation of fluorescent markers like H33342 and rhodamine 123, in the absence or presence of specific inhibitors (e.g., verapamil) [37]. It has been shown that stem cells from diverse sources show a high activity of efflux pumps of the ABC transporters, such as P-gp and Bcrp, and thus exclude the above mentioned dyes [36,53]. Particularly, with H33342 staining, a specific cell population can be sorted, the so-called "side-population" [51,52]. This portion is enriched in "repopulating" stem cells, which comprise 0.05% of the bone marrow cells [53]. In turn, most differentiated cells undergo down regulation of the encoding genes and thus show high dye-staining [36].

Invertebrate and vertebrate ABCs share structural features [37]. In this work, we found two hemocyte subpopulations with different ABC transporters activities (Fig. 6). Most circulating hemocytes (99%) showed high H33342-staining and, thus, may correspond to mature circulating hemocytes with low dye-efflux activity. A small subpopulation (0.06–0.12%) showed low H33342 dye staining, suggesting a high ABC transporter activity which was inhibited by 100 and 500 μM verapamil, as that reported for the "side-population" of humans and mice [52,53]. This small population may be interpreted as circulating quiescent progenitor cells. Furthermore, the sensitivity of H33342 efflux to verapamil indicates that a P-gp–like efflux transporter [69] may be involved in these stem-like hemocytes.

5. Conclusions and future research

In summary, our results show that adult hemocytes can proliferate in the blood of recipient *P. canaliculata* individuals and, to our knowledge,

this work represents to the first successful transfer of CFSE-labeled hemocytes in a gastropod. We also describe, for the first time, circulating hemocytes in all phases of the cell cycle in *P. canaliculata*. We found evidence for quiescent, non-cycling small hemocytes with low complexity-granularity and RNA content, as well as active-cycling cells with high DNA and RNA contents. Further, our studies suggest that a circulating subpopulation of hemocytes retains functional features of stem cells, i.e., a low mitochondrial membrane potential and high H33342 dye-efflux activity.

Taken together, our data supports the hypothesis of a circulating stem cell population in *P. canaliculata*, which would add to our earlier findings of hematopoiesis in the kidney hemocyte islets and the lung nodules, among others. Importantly, this would open avenues to investigate molecular markers linked to functions in this system of progenitor cells, which may be used for comparative studies within the highly diverse clade Caenogastropoda.

CRediT authorship contribution statement

Cristian Rodriguez: Methodology, Validation, Formal analysis, Investigation, Writing - review & editing, Visualization, Funding acquisition. **Valeska Simon:** Data curation, Visualization. **Paulette Conget:** Conceptualization, Supervision, Project administration, Funding acquisition. **Israel A. Vega:** Conceptualization, Methodology, Formal analysis, Investigation, Resources, Writing - original draft, Visualization, Funding acquisition.

Declaration of competing interest

The authors have declared that no competing interests exist.

Acknowledgments

We thank Mrs. Anita Diaz and Silvia Diaz for assistance with animal care and Mrs. Paola Ramos for her assistance in the maintenance of the culture room, laminar flow, and making of the culture media.

Appendix A. Supplementary data

Supplementary data to this article can be found online at https://doi.org/10.1016/j.fsi.2020.09.026.

Funding

This work was supported by a grant for researchers from CONICET (2009–2010) and grants from Secretaría de Investigación, Internacionales y Posgrado (SIIP), Universidad Nacional de Cuyo, Mendoza, Argentina [grant numbers M086 and 06/J523]. The funders had no role in study design, data collection and analysis, decision to publish, or preparation of the manuscript.

References

[1] K.A. Hayes, R.L. Burks, A. Castro-Vazquez, P.C. Darby, H. Heras, P.R. Martín, J.-W. Qiu, S.C. Thiengo, I.A. Vega, T. Wada, Y. Yusa, S. Burela, M.P. Cadierno, J. A. Cueto, F.A. Dellagnola, M.S. Dreon, M.V. Frassa, M. Giraud-Billoud, M.S. Godoy, S. Ituarte, E. Koch, K. Matsukura, M.Y. Pasquevich, C. Rodriguez, L. Saveanu, M. E. Seuffert, E.E. Strong, J. Sun, N.E. Tamburi, M.J. Tiecher, R.L. Turner, P. L. Valentine-Darby, R.H. Cowie, Insights from an integrated view of the biology of apple snails (Caenogastropoda: Ampullariidae), Malacologia 58 (2015) 245–302.

[2] F. Horgan, The ecophysiology of apple snails in rice: implications for crop management and policy, Ann. Appl. Biol. 172 (2018) 245–267.

[3] R. Cowie, *Angiostrongylus cantonensis*: agent of a sometimes fatal globally emerging infectious disease (rat lungworm disease), ACS Chem. Neurosci. 8 (2017) 2102.

[4] S. Lv, Y.-H. Guo, H.M. Nguyen, M. Sinuon, S. Sayasone, N.C. Lo, X.-N. Zhou, J. R. Andrews, Invasive *Pomacea* snails as important intermediate hosts of *Angiostrongylus cantonensis* in Laos, Cambodia and Vietnam: implications for outbreaks of eosinophilic meningitis, Acta Trop. 183 (2018) 32–35.

[5] L. Song, X. Wang, Z. Yang, Z. Lv, Z. Wu, *Angiostrongylus cantonensis* in the vector snails *Pomacea canaliculata* and *Achatina fulica* in China: a meta-analysis, Parasitol. Res. 115 (2016) 913–923.

[6] A. Accorsi, S. Benatti, E. Ross, M. Nasi, D. Malagoli, A prokineticin-like protein responds to immune challenges in the gastropod pest *Pomacea canaliculata*, Dev. Comp. Immunol. 72 (2017) 37–43.

[7] A. Accorsi, L. Bucci, M. de Eguileor, E. Ottaviani, D. Malagoli, Comparative analysis of circulating hemocytes of the freshwater snail *Pomacea canaliculata*, Fish Shellfish Immunol. 34 (2013) 1260–1268.

[8] A. Accorsi, E. Ottaviani, D. Malagoli, Effects of repeated hemolymph withdrawals on the hemocyte populations and hematopoiesis in *Pomacea canaliculata*, Fish Shellfish Immunol. 38 (2014) 56–64.

[9] F. Boraldi, F.D. Lofaro, A. Accorsi, E. Ross, D. Malagoli, Toward the molecular deciphering of *Pomacea canaliculata* immunity: first proteomic analysis of circulating hemocytes, Proteomics 19 (2019) 1800314.

[10] J.A. Cueto, C. Rodriguez, I.A. Vega, A. Castro-Vazquez, Immune defenses of the invasive apple snail *Pomacea canaliculata* (Caenogastropoda, Ampullariidae): phagocytic hemocytes in the circulation and the kidney, PLoS One 10 (2015), e0123964, https://doi.org/10.1371/journal.pone.0123964.

[11] J.A. Cueto, I.A. Vega, A. Castro-Vazquez, Multicellular spheroid formation and evolutionary conserved behaviors of apple snail hemocytes in culture, Fish Shellfish Immunol. 34 (2013) 443–453.

[12] C. Rodriguez, G.I. Prieto, I.A. Vega, A. Castro-Vazquez, Assessment of the kidney and lung as immune barriers and hematopoietic sites in the invasive apple snail *Pomacea canaliculata*, PeerJ 6 (2018) e5789.

[13] C. Rodriguez, G.I. Prieto, I.A. Vega, A. Castro-Vazquez, Functional and evolutionary perspectives on gill structures of an obligate air-breathing, aquatic snail, PeerJ 7 (2019), e7342.

[14] J. Cueto, *Pomacea canaliculata* (Architaenioglossa, Ampullariidae): La hemolinfa y sus células. PhD Thesis, Universidad Nacional de Cuyo, 2011.

[15] E. Ottaviani, Tissue distribution and levels of natural and induced serum lysozyme immunoreactive molecules in a freshwater snail, Tissue Cell 23 (1991) 317–324.

[16] J.A. Pickett, J.M. Edwardson, Compound exocytosis: mechanisms and functional significance, Traffic 7 (2006) 109–116.

[17] E. Pila, J. Sullivan, X. Wu, J. Fang, S. Rudko, M. Gordy, P. Hanington, Haematopoiesis in molluscs: a review of haemocyte development and function in gastropods, cephalopods and bivalves, Dev. Comp. Immunol. 58 (2016) 119–128.

[18] V. Hartenstein, Blood cells and blood cell development in the animal kingdom, Annu. Rev. Cell Dev. Biol. 22 (2006) 677–712.

[19] K. Lie, D. Heyneman, P. Yau, The origin of amebocytes in *Biomphalaria glabrata*, J. Parasitol. 61 (1975) 574–576.

[20] C.-T. Pan, Studies on the host-parasite relationship between *Schistosoma mansoni* and the snail *Australorbis glabratus*, Am. J. Trop. Med. Hyg. 14 (1965) 931–976.

[21] R.A. Rohr, S.B. Amato, Localização e caracterização de tecidos hematopoiéticos em duas espécias de gastrópodes Stylommatophora, Revista Eletrônica de Biologia (REB) (2014) 43–50, 1983-7682 7.

[22] D. Rondelaud, D. Barthe, The development of the amoebocyte-producing organ in *Lymnaea truncatula* Müller infected by *Fasciola hepatica* L, Z. für Parasitenkd. 65 (1981) 331–341.

[23] L. Ruellan, D. Rondelaud, Lamellar structure of the amoebocyte-producing tissue in *Lymnaea truncatula* infected with *Fasciola hepatica*, Parasitol. Res. 78 (1992) 270–272.

[24] J.T. Sullivan, Hematopoiesis in three species of gastropods following infection with *Echinostoma paraensei* (Trematoda: echinostomatidae), Trans. Am. Microsc. Soc. 107 (1988) 355–361.

[25] J.T. Sullivan, T.C. Cheng, K.H. Howland, Mitotic responses of the anterior pericardial wall of *Biomphalaria glabrata* (Mollusca) subjected to challenge, J. Invertebr. Pathol. 44 (1984) 114–116.

[26] T. Sminia, Haematopoiesis in the freshwater snail *Lymnaea stagnalis* studied by electron microscopy and autoradiography, Cell Tissue Res. 150 (1974) 443–454.

[27] T. Sminia, W. Van der Knaap, L. Van Asselt, Blood cell types and blood cell formation in gastropod molluscs, Dev. Comp. Immunol. 7 (1983) 665–668.

[28] W. Van der Knaap, C. Adema, T. Sminia, Invertebrate blood cells: morphological and functional aspects of the haemocytes in the pond snail *Lymnaea stagnalis*, Comparative Haematology International 3 (1993) 20–26.

[29] A.B. Lyons, C.R. Parish, Determination of lymphocyte division by flow cytometry, J. Immunol. Methods 171 (1994) 131–137.

[30] P.A. Conget, J.J. Minguell, Phenotypical and functional properties of human bone marrow mesenchymal progenitor cells, J. Cell. Physiol. 181 (1999) 67–73.

[31] R. Nunez, DNA measurement and cell cycle analysis by flow cytometry, Curr. Issues Mol. Biol. 3 (2001) 67–70.

[32] Z. Darzynkiewicz, Differential staining of DNA and RNA in intact cells and isolated cell nuclei with acridine orange, Methods Cell Biol. 33 (1990) 285–298.

[33] A. Cossarizza, S. Salvioli, Flow cytometric analysis of mitochondrial membrane potential using JC-1, Current Protocols in Cytometry (2001), 9.14.11-19.14.17.

[34] S.T. Smiley, M. Reers, C. Mottola-Hartshorn, M. Lin, A. Chen, T.W. Smith, G. Steele, L.B. Chen, Intracellular heterogeneity in mitochondrial membrane potentials revealed by a J-aggregate-forming lipophilic cation JC-1, Proc. Natl. Acad. Sci. Unit. States Am. 88 (1991) 3671–3675.

[35] M. Sukumar, J. Liu, G.U. Mehta, S.J. Patel, R. Roychoudhuri, J.G. Crompton, C. A. Klebanoff, Y. Ji, P. Li, Z. Yu, Mitochondrial membrane potential identifies cells with enhanced stemness for cellular therapy, Cell Metabol. 23 (2016) 63–76.

[36] S.D.P.W.M. de Jonge-Peeters, F. Kuipers, E.G.E. de Vries, E. Vellenga, ABC transporter expression in hematopoietic stem cells and the role in AML drug resistance, Crit. Rev. Oncol. Hematol. 62 (2007) 214–226.

[37] C.-B. Jeong, H.-S. Kim, H.-M. Kang, J.-S. Lee, ATP-binding cassette (ABC) proteins in aquatic invertebrates: evolutionary significance and application in marine ecotoxicology, Aquat. Toxicol. 185 (2017) 29–39.
[38] D. Kessel, W.T. Beck, D. Kukuruga, V. Schulz, Characterization of multidrug resistance by fluorescent dyes, Canc. Res. 51 (1991) 4665–4670.
[39] J. Nicholson, D. Stein, T. Mui, R. Mack, M. Hubbard, T. Denny, Evaluation of a method for counting absolute numbers of cells with a flow cytometer, Clin. Diagn. Lab. Immunol. 4 (1997) 309–313.
[40] Z. Darzynkiewicz, S. Bruno, G. Del Bino, W. Gorczyca, M. Hotz, P. Lassota, F. Traganos, Features of apoptotic cells measured by flow cytometry, Cytometry 13 (1992) 795–808.
[41] A.B. Lyons, S.J. Blake, K.V. Doherty, Flow cytometric analysis of cell division by dilution of CFSE and related dyes, Current Protocols in Cytometry 64 (2013) 9–11.
[42] L. de Abreu Costa, M. Henrique Fernandes Ottoni, M.G. dos Santos, A.B. Meireles, V. Gomes de Almeida, W. de Fátima Pereira, B. Alves de Avelar-Freitas, G. Eustáquio Alvim Brito-Melo, Dimethyl sulfoxide (DMSO) decreases cell proliferation and TNF-α, IFN-γ, and IL-2 cytokines production in cultures of peripheral blood lymphocytes, Molecules 22 (2017) 1789.
[43] V. Fretter, A. Graham, British Prosobranch Molluscs. Their Functional Anatomy and Ecology., Ray Society, 1962.
[44] D. Sakharov, K.S.- Rózsa, Defensive behaviour in the pond snail, *Lymnaea stagnalis*: the whole body withdrawal associated with exsanguination, Acta Biol. Hung. 40 (1988) 329–341.
[45] B. Asquith, C. Debacq, A. Florins, N. Gillet, T. Sanchez-Alcaraz, A. Mosley, L. Willems, Quantifying lymphocyte kinetics in vivo using carboxyfluorescein diacetate succinimidyl ester, Proc. R. Soc. Lond. B Biol. Sci. 273 (2006) 1165–1171.
[46] C. Debacq, N. Gillet, B. Asquith, M.T. Sanchez-Alcaraz, A. Florins, M. Boxus, I. Schwartz-Cornil, M. Bonneau, G. Jean, P. Kerkhofs, Peripheral blood B-cell death compensates for excessive proliferation in lymphoid tissues and maintains homeostasis in bovine leukemia virus-infected sheep, J. Virol. 80 (2006) 9710–9719.
[47] M. Reers, T.W. Smith, L.B. Chen, J-aggregate formation of a carbocyanine as a quantitative fluorescent indicator of membrane potential, Biochemistry 30 (1991) 4480–4486.
[48] F. Sivandzade, A. Bhalerao, L. Cucullo, Analysis of the mitochondrial membrane potential using the cationic JC-1 dye as a sensitive fluorescent probe, Bio-Protocol 9 (2019) e3128.
[49] C. Mantel, S. Messina-Graham, H.E. Broxmeyer, Upregulation of nascent mitochondrial biogenesis in mouse hematopoietic stem cells parallels upregulation of CD34 and loss of pluripotency: a potential strategy for reducing oxidative risk in stem cells, Cell Cycle 9 (2010) 2008–2017.
[50] I. Bertoncello, B. Williams, Hematopoietic stem cell characterization by Hoechst 33342 and rhodamine 123 staining, in: T.S. Hawley, R.G. Hawley (Eds.), Flow Cytometry Protocols. Methods in Molecular Biology, Humana Press, 2004, pp. 181–200.
[51] J.E. Oates, B.R. Grey, S.K. Addla, J.D. Samuel, C.A. Hart, V.A. Ramani, M.D. Brown, N.W. Clarke, Hoechst 33342 side population identification is a conserved and unified mechanism in urological cancers, Stem Cell. Dev. 18 (2009) 1515–1522.
[52] M.A. Goodell, M. Rosenzweig, H. Kim, D.F. Marks, M. DeMaria, G. Paradis, S. A. Grupp, C.A. Sieff, R.C. Mulligan, R.P. Johnson, Dye efflux studies suggest that hematopoietic stem cells expressing low or undetectable levels of CD34 antigen exist in multiple species, Nat. Med. 3 (1997) 1337–1345.
[53] S. Zhou, J.D. Schuetz, K.D. Bunting, A.-M. Colapietro, J. Sampath, J.J. Morris, I. Lagutina, G.C. Grosveld, M. Osawa, H. Nakauchi, The ABC transporter Bcrp1/ABCG2 is expressed in a wide variety of stem cells and is a molecular determinant of the side-population phenotype, Nat. Med. 7 (2001) 1028–1034.
[54] F. Yousif, S. Blähser, G. Lämmler, The cellular responses in *Marisa cornuarietis* experimentally infected with *Angiostrongylus cantonensis*, Parasitol. Res. 62 (1980) 179–190.
[55] A.S. Bhunia, S. Mukherjee, N.S. Bhunia, M. Ray, S. Ray, Immunological resilience of a freshwater Indian mollusc during aestivation and starvation, Aquaculture Reports 3 (2016) 1–11.
[56] F. Buttgereit, G.-R. Burmester, M.D. Brand, Bioenergetics of immune functions: fundamental and therapeutic aspects, Immunol. Today 21 (2000) 194–199.
[57] C.D. Folmes, T.J. Nelson, A. Martinez-Fernandez, D.K. Arrell, J.Z. Lindor, P. P. Dzeja, Y. Ikeda, C. Perez-Terzic, A. Terzic, Somatic oxidative bioenergetics transitions into pluripotency-dependent glycolysis to facilitate nuclear reprogramming, Cell Metabol. 14 (2011) 264–271.
[58] A. Prigione, B. Fauler, R. Lurz, H. Lehrach, J. Adjaye, The senescence-related mitochondrial/oxidative stress pathway is repressed in human induced pluripotent stem cells, Stem Cell. 28 (2010) 721–733.
[59] X. Xu, S. Duan, F. Yi, A. Ocampo, G.-H. Liu, J.C.I. Belmonte, Mitochondrial regulation in pluripotent stem cells, Cell Metabol. 18 (2013) 325–332.
[60] W. Zhou, M. Choi, D. Margineantu, L. Margaretha, J. Hesson, C. Cavanaugh, C. A. Blau, M.S. Horwitz, D. Hockenbery, C. Ware, HIF1α induced switch from bivalent to exclusively glycolytic metabolism during ESC-to-EpiSC/hESC transition, EMBO J. 31 (2012) 2103–2116.
[61] E. Ansó, S.E. Weinberg, L.P. Diebold, B.J. Thompson, S. Malinge, P.T. Schumacker, X. Liu, Y. Zhang, Z. Shao, M. Steadman, The mitochondrial respiratory chain is essential for haematopoietic stem cell function, Nat. Cell Biol. 19 (2017) 614.
[62] M.Z. Ratajczak, J. Ratajczak, M. Kucia, Very small embryonic-like stem cells (VSELs) an update and future directions, Circ. Res. 124 (2019) 208–210.
[63] J. Facucho-Oliveira, J.S. John, The relationship between pluripotency and mitochondrial DNA proliferation during early embryo development and embryonic stem cell differentiation, Stem Cell Reviews and Reports 5 (2009) 140–158.
[64] T. Lonergan, B. Bavister, C. Brenner, Mitochondria in stem cells, Mitochondrion 7 (2007) 289–296.
[65] C. Nesti, L. Pasquali, M. Mancuso, G. Siciliano, The role of mitochondria in stem cell biology, in: V.K. Rajasekhar, M.C. Vemuri (Eds.), Regulatory Networks in Stem Cells. Stem Cell Biology and Regenerative Medicine, Humana Press, 2009, pp. 137–143.
[66] S.T. Suhr, E.A. Chang, J. Tjong, N. Alcasid, G.A. Perkins, M.D. Goissis, M. H. Ellisman, G.I. Perez, J.B. Cibelli, Mitochondrial rejuvenation after induced pluripotency, PloS One 5 (2010), e14095.
[67] M. Achard, M. Baudrimont, A. Boudou, J. Bourdineaud, Induction of a multixenobiotic resistance protein (MXR) in the Asiatic clam *Corbicula fluminea* after heavy metals exposure, Aquat. Toxicol. 67 (2004) 347–357.
[68] K.E. Whalen, E.E. Sotka, J.V. Goldstone, M.E. Hahn, The role of multixenobiotic transporters in predatory marine molluscs as counter-defense mechanisms against dietary allelochemicals, Comp. Biochem. Physiol. C Toxicol. Pharmacol. 152 (2010) 288–300.
[69] P.M. Chaudhary, I.B. Roninson, Expression and activity of P-glycoprotein, a multidrug efflux pump, in human hematopoietic stem cells, Cell 66 (1991) 85–94.